Supporting Information

A Cu-dopped Alloy Layer Guiding Li Uniform Deposition on Li-LLZO Interface under High Current Density

Xia He, Fei Yan, Mingyuan Gao, Yunjing Shi, Guanglong Ge, Bo Shen, Jiwei Zhai*

Key Laboratory of Advanced Civil Engineering Materials of Ministry of Education, Functional Materials Research Laboratory, School of Materials Science & Engineering, Tongji University, 4800 Caoan Road, Shanghai 201804, China

*Corresponding author: *Jiwei Zhai*

4800 Caoan Road, Shanghai, 201804, China

Phone:86+13122389697

E-mail address: apzhai@tongji.edu.cn

A table of contents

Digital photo; XRD pattern; Illustration of magnetron co-sputtering; SEM images; XPS spectra; Voltage profiles; Cycling performance.

Tables

Figures

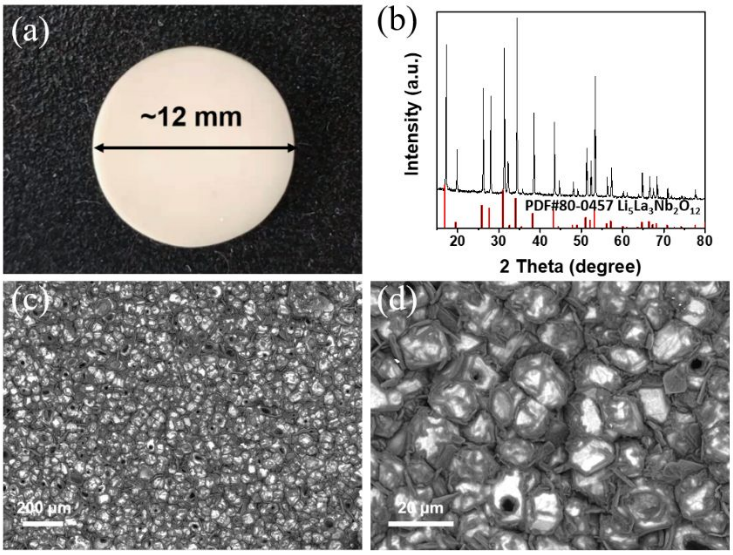

Figure S1. The property of LLZTO pellet. (a) the digital photo of as-prepared LLZTO pellet, (b) XRD pattern of prepared garnet electrolyte, (c)-(d) the SEM image of the top surface of untreated LLZTO pellet.

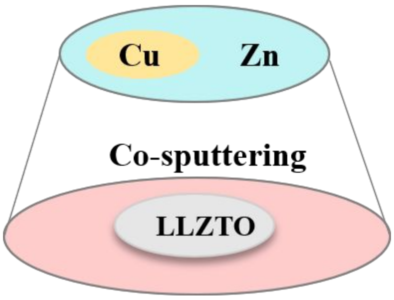

Figure S2. The illustration of magnetron co-sputtering of Zn and Cu.

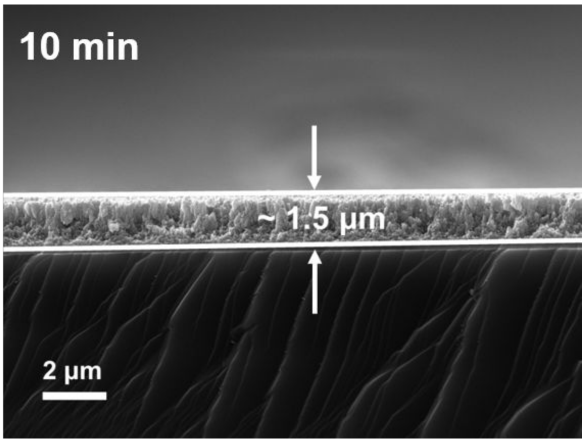

Figure S3. The thickness of the Zn-Cu composite layer coated on Silicon substrate after 10 min. As calculated, the sputtering speed is about 150 nm/min.

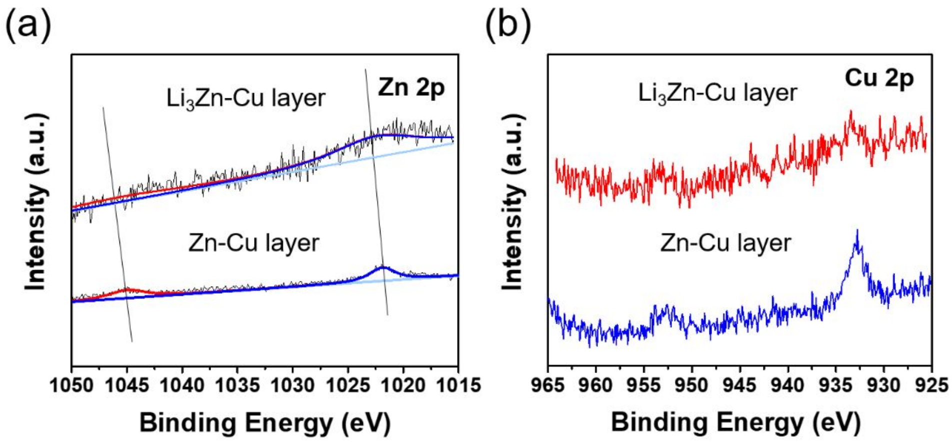

Figure S4. XPS spectra of Zn-Cu glass substrate and Li_3Zn-Cu glass substrate, (a) Zn 2p, (b) Cu 2p.

From the XPS spectra, the peaks at the binding energies of 1021.8 and 1044.9 eV, corresponding to Zn $2p_{3/2}$ and $2p_{1/2}$, shifted to 1022.3 eV and 1045.2. The peaks at the binding energies of 932.7 and 952.3 kept at the same position. The XPS spectra exhibited that the Zn alloyed with Li, and the Cu nanoparticles combined in the alloy.

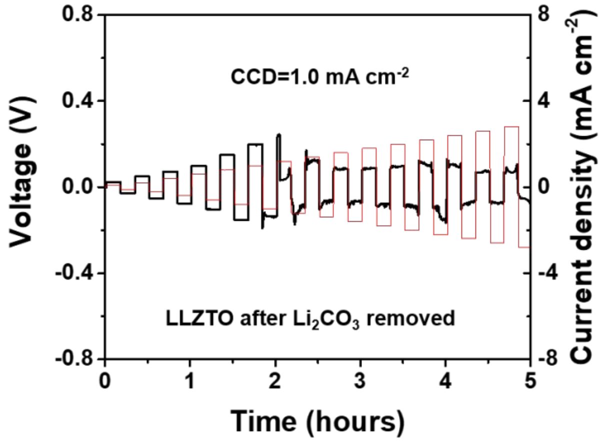

Figure S5. Voltage profiles at increased current densities with constant capacity of 0.1 mA cm^{-2} in Li/ LLZTO/Li.

Table S1. Comparison of state-of -the -art CCD values with cycling protocols for the oxide electrolytes.

Method-electrolyte	**CCD (mA cm^{-2}) /duration time(per cycle)**	**Areal capacity (mAh cm^{-2})**	**Temperature(°C)/ reference**
Li_2CO_3 free LLZO	0.9/30min	0.45	60/ [1]
ZnO-LLZO	0.1/<0.01	-	25/ [2]
Al_2O_3-LLZO	0.2/30min	0.1	25/ [3]
Li-C_3N_4-LLZO	1.5/10min	0.25	25/ [4]
Li-Ag coated LLZO	0.75/2h	1.5	25/ [5]
Li_3OCl coating LLZO	0.05/1h	0.05	25/ [6]
TVD-carbon-LLZO	1.2/30min	0.6	25/ [7]
Si CVD LLZO	0.2/5min	0.0167	25/ [8]

Au sputtered LLZO	0.8/30min	0.4	50/ [9]
Pencil drawing interface LLZO	0.3/1h	0.3	25/ [10]
Li-Al alloy LLZO	2.3/10min	0.4	60/ [11]
	1.2/10min	0.2	25/ [11]
Cu-dopped Li_3Zn-LLZTO	2.8/15min	0.7	25/This work

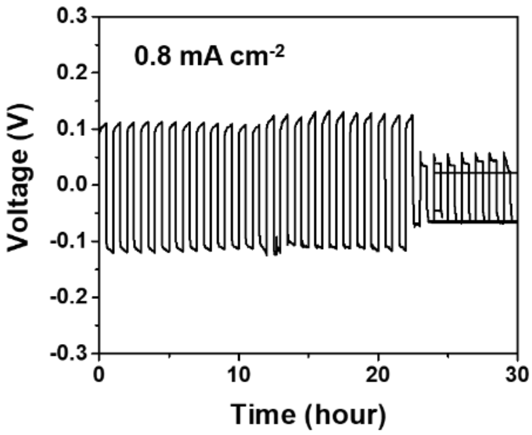

Figure S6. The cycling performance of Li symmetric cell equipped with Zn-modified SSEs at a high current density.

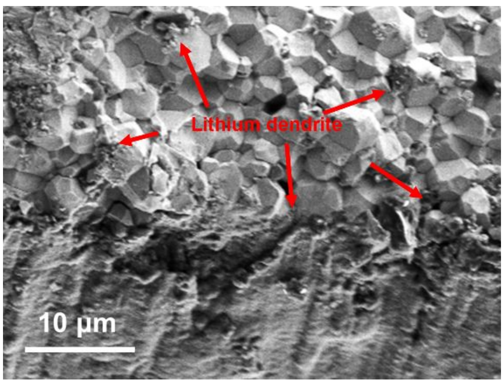

Figure S7. SEM image of Zn-modified interface after cycling for 30 hours at 0.8 mA cm^{-2}.

Reference

[1] Wu, J. F.; Pu, B. W.; Wang, D.; Shi, S. Q.; Zhao, N.; Guo, X.; Guo, X.; In Situ Formed Shields Enabling Li_2CO_3-Free Solid Electrolytes: A New Route to Uncover the Intrinsic Lithiophilicity of Garnet Electrolytes for Dendrite-Free Li-Metal Batteries. ACS Appl. Mater. Interfaces 2019, 11, 898– 905.

[2] Wang, C.; Gong, Y.; Liu, B.; Fu, Y.; Yao, K.; Hitz, E.; Li, Y.; Dai, J.; Xu, S.; Luo, W.; Wachsman, E. D.; Hu, L.; Conformal, Nanoscale ZnO Surface Modification of Garnet-Based Solid-State Electrolyte for Lithium Metal Anodes. Nano Lett. 2017, 17, 565– 571.

[3] Han, X.; Gong, Y.; Fu, K. K.; He, X.; Hitz, G. T.; Dai, J.; Pearse, A.; Liu, B.; Wang, H.; Rubloff, G.; Mo, Y.; Thangadurai, V.; Wachsman, E. D.; Hu, L.; Negating Interfacial Impedance in Garnet-Based Solid-State Li Metal Batteries. Nat. Mater. 2017, 16, 572– 579.

[4] Huang, Y.; Chen, B.; Duan, J.; Yang, F.; Wang, T.; Wang, Z.; Yang, W.; Hu, C.; Luo, W.; Huang, Y.; Angew. Chem. Int. Ed. 2020, 59, 3699– 3704.

[5] Cai, M.; Lu, Y.; Su, J.; Ruan, Y.; Chen, C.; Chowdari, B. V. R.; Wen, Z.; Graphitic Carbon Nitride (g-C_3N_4): An Interface Enabler for Solid-State Lithium Metal Batteries. ACS Appl. Mater. Interfaces 2019, 11, 35030– 35038.

[6] Tian, Y.; Ding, F.; Zhong, H.; Liu, C.; He, Y.-B.; Liu, J.; Liu, X.; Xu, Q.; $Li_{6.75}La_3Zr_{1.75}Ta_{0.25}O_{12}$@ amorphous Li_3OCl composite electrolyte for solid state lithium-metal batteries. Energy Storage Mater. 2018, 14, 49– 57.

[7] Feng, W.; Dong, X.; Zhang, X.; Lai, Z.; Li, P.; Wang, C.; Wang, Y.; Xia, Y.; Li/Garnet Interface Stabilization by Thermal-Decomposition Vapor Deposition of an Amorphous Carbon Layer. Angew. Chem., Int. Ed. 2020, 59, 5346– 5349.

[8] Luo, W.; Gong, Y.; Zhu, Y.; Fu, K. K.; Dai, J.; Lacey, S. D.; Wang, C.; Liu, B.; Han, X.; Mo, Y.; Wachsman, E. D.; Hu, L.; Transition From Superlithiophobicity to Superlithiophilicity of Garnet Solid-State Electrolyte. J. Am. Chem. Soc. 2016, 138, 12258–12262.

[9] Tsai, C. L.; Roddatis, V.; Chandran, C. V.; Ma, Q.; Uhlenbruck, S.; Bram, M.; Heitjans, P.; Guillon, O.; $Li_7La_3Zr_2O_{12}$ Interface Modification for Li Dendrite Prevention. ACS Appl. Mater. Interfaces 2016, 8, 10617– 106026.

[10] Shao, Y.; Wang, H.; Gong, Z.; Wang, D.; Zheng, B.; Zhu, J.; Lu, Y.; Hu, Y.-S.; Guo, X.; Li, H.; Huang, X.; Yang, Y.; Nan, C.-W.; Chen, L.; Drawing A Soft Interface: An Effective Interfacial Modification Strategy for Garnet-Type Solid-State Li Batteries. ACS Energy Lett. 2018, 3, 1212– 1218.

[11] Lu, Y.; Huang, X.; Ruan, Y.; Wang, Q.; Kun, R.; Yang, J.; Wen, Z.; An In Situ Element Ppermeation Constructed High Endurance Li–LLZO Interface at High Current Densities. J. Mater. Chem. A 2018, 6, 18853– 18858.